Supplementary Information (SI) for Journal of Materials Chemistry C.
This journal is © The Royal Society of Chemistry 2025

High efficiency sulfamethoxazole degradation enabled by chlorinated D-A scheme organic photocatalyst

Nannan Geng,[a,c] Linji Yang,[a,c] Yuchen Wang,[a] Ciyuan Huang,[a] Guowei Geng,[a] Liangsheng Chen,[a] Ke Sun,[b] Tao Liu,[a,b*]

a. N. Geng, L. Yang,Y. Wang, C. Huang, G. Geng, L. Chen, Prof. K. Sun, Prof. T. Liu, Guangxi Key Laboratory of Processing for Non-ferrous Metals and Featured Materials, MOE Key Laboratory of New Processing Technology for Non-ferrous Metals and Materials, School of Chemistry and Chemical Engineering, School of Resources, Environment and Materials, Guangxi University, Nanning 530004, China.
Email: liutaozhx@gxu.edu.cn

b. Prof. K. Sun, Prof. T. Liu,
Department of Biochemistry and Cell Biology, YouJiang Medical University for Nationalities, Baise City, Guangxi Zhuang Autonomous Region 533000, China.

c. These authors contributed equally.

1. Materials and methods

1.1. Chemicals and reagents

Coconut Shell Carbon (CSC) was purchased from Science Compass (China). Sulfamethoxazole (SMX), 1,4-Benzoquinone (BQ), KBr, Sodium oxalate ($Na_2C_2O_4$), isopropyl alcohol (IPA), Na_2CO_3, Na_2SO_4, and NaOH were purchased from Aladdin (Shanghai, China) without further purification.

1.2. Preparation of catalyst

The catalysts were prepared by static-loading.

(J71:IT-2Cl)@CSC: 7.5 mg of J71 and IT-2Cl were weighed separately, dissolved in 20 ml of chloroform, and stirred airtight for 12 hours. Weigh 8g of coconut shell carbon in a surface dish. After stirring, pour the chloroform solution into the surface dish. Place the surface dish on a 50°C thermostatic heating table and let it stand for 24 hours in a fume hood.

(J71:IT-4Cl)@CSC: Same method as described above.

Fig. S1. Preparation of catalyst((J71:IT-2Cl)@CSC).

1.3. Characterization of the sample

The morphology of the prepared samples was carried out via scanning electron microscope (SEM, Zeiss Sigma 300), and the elemental distributions of catalyst were determined by energy-dispersive spectrometry (EDS)-elemental mapping analysis. UV-vis diffuse reflectance spectra (DRS) were recorded on a SHIMADZU UV-2600i＆ISR-2600Plus.Surface Photovoltaic Spectroscopy (SPV) was measured by PL-SPV/IPCE1000 Stable surface photovoltage spectrometer. The Brunner Emmet Teller (BET, ASAP 2460 Version 3.01) was employed on the pore size and specific surface area of materials. Photoluminescence (PL) spectra and Time-Resolved Photoluminescence (TRPL) were measured by Fluorescence Spectrophotometer (F-7000, Hitachi, Japan). Transient photo-current responses and photocurrent and electrochemical impedance spectroscopy (EIS) were tested by an electrochemical

workstation (CHI-660E, Zhenhua, China). The electrolyte is Na2SO4 solution (0.5 M). ITO coated with photocatalyst served as the working electrode, Ag/AgCl electrode as the reference electrode, and Pt as the counter electrode.

1.4. Photocatalytic degradation of SMX

The photoactivity of catalysts was estimated by degrading SMX under visible light irradiation. In the photocatalytic experiments, 100 mg of photocatalyst was immersed in 50 mL of aqueous SMX solution (20 mg/L), which was then placed under the irradiation of a 300 W xenon lamp with a 420 nm cutoff filter. At given 10 min interval, 4 mL of solutions were gathered. The pollution concentration was measured by the UV-vis spectrophotometer at absorption wavelength of 266 nm.

1.5. Analysis of intermediate products

The electron spin resonance (ESR) signals of spin-trapped radicals were studied on a Bruker model ESR JESFA200 spectrometer using spin-trap reagent DMPO in water and methanol, respectively.

The total organic carbon (TOC) analyzer (TOC-L, Shimadzu) was used to analyze the mineralization extent of SMX. The photodegradation intermediates of SMX were determined by a high-performance liquid chromatograph-tandem mass spectrometer (HPLC-MS system, Thermo, America).

1.6 Photocatalyst loading process

J71:IT-2Cl (1:1 weight ratio), J71:IT-4Cl (1:1 weight ratio) were loaded on the surface of coconut shell carbon at a weight ratio of 1:400.

1.7 Decay time fitting method

Decay time double-exponential fitting formula:

$$I(x) = I_0 + Sum(i \geq 1)A(i) * \exp(-x / T(i))$$

Where $\mathbf{T_1}$ and $\mathbf{T_2}$ are the fitted lifetimes and $\boldsymbol{A_1}$ and $\boldsymbol{A_2}$ are the weighting parameters. The average lifetime (the finite portion) is defined as:

$$\boldsymbol{T_{av}} = \frac{\boldsymbol{A_1 * T_1^2 + A_2 * T_2^2}}{\boldsymbol{A_1 * T_1 + A_2 * T_2}}$$

The weighting parameters of $\boldsymbol{A_{1/2}}$% are calculated as:

$$\boldsymbol{A}_{1/2}\% = \frac{\boldsymbol{A}_{1/2}}{\boldsymbol{A}_1 + \boldsymbol{A}_2} \times 100\%$$

1.8 Computational details

The density functional theory (DFT) was performed with the Materials Studio. The generalised gradient approximation (GGA) Perdew-Burke-Ernzerhof (PBE) was used for correlation functions such as HOMO/LUMO and Fukui functions. The max step size of the system was regulated to 0.3 Å per atom and the max number of cycles was 500. The DFT-D method is used in all calculations to describe weak interactions such as van der Waals forces. The core treatment was chosen as DFT Semi-core Pseudopots. Furthermore, the calculations were carried out until convergence, which was achieved by a maximum force per atom of less than 0.002 eV/Å and an energy of less than 1.0×10^{-5} Ha.

2. Results and discussion

As shown in the **Fig. S2**, the neat IT-4Cl film shows pronounced (010) π–π stacking peak located at q = 1.79 $Å^{-1}$ in the out-of-plane (OOP) direction corresponding to a distance of 3.51 Å. Meanwhile, it also exhibited (100) lamellar peaks located at q = 0.37 $Å^{-1}$ in the in-plane (IP) profile with a d-spacing of 17.0 Å. The results indicate that the IT-4Cl prefers increased crystallinity and a face-on orientation. The replacement of fluorine atoms by chlorine atoms increases the dipole moments of the end groups from 2.26 to 2.77 D(**Fig. S3**), and thus enhances the the intramolecular charge-transfer (ICT) effect in IT-4Cl and IT-2Cl[1].

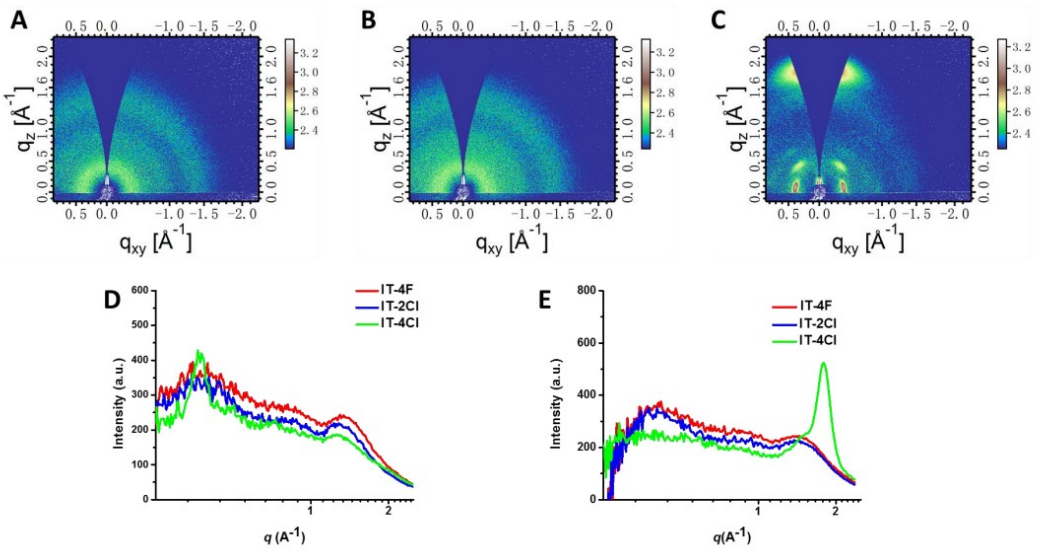

Fig. S2. The GIWAXS 2D pattern of the pristine films of (A) IT-4F, (B) IT-2Cl and (C) IT-4Cl. In-plane (IP) and out of plane (OOP) line profiles of the pristine films.[1]

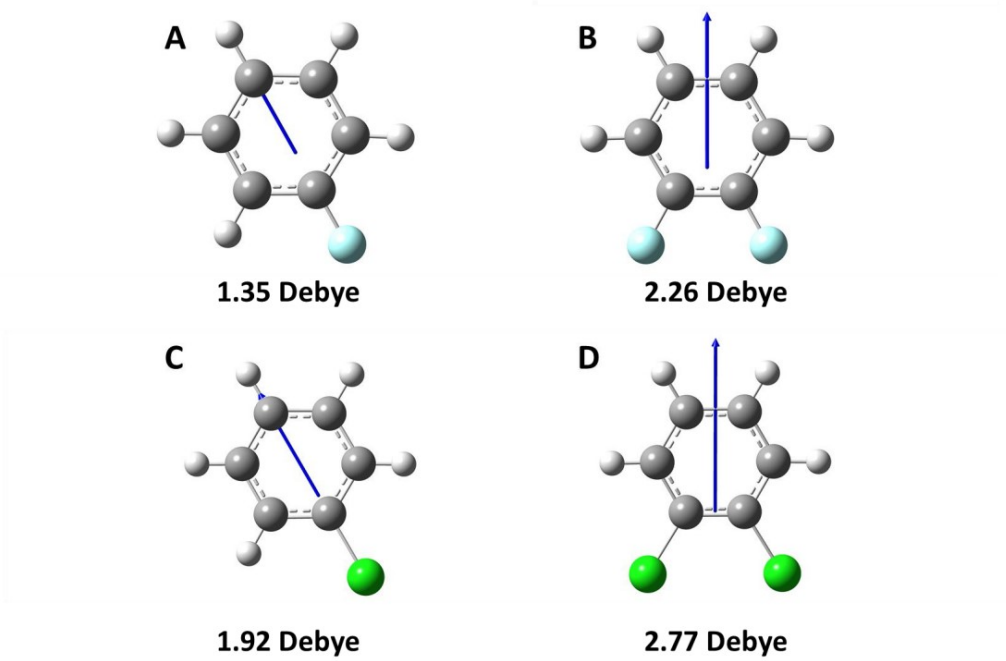

Fig. S3. The dipole moments of (A) chlorobenzene, (B) dichlorobenzene, (C) fluorobenzene and (D) difluorobenzene.[1]

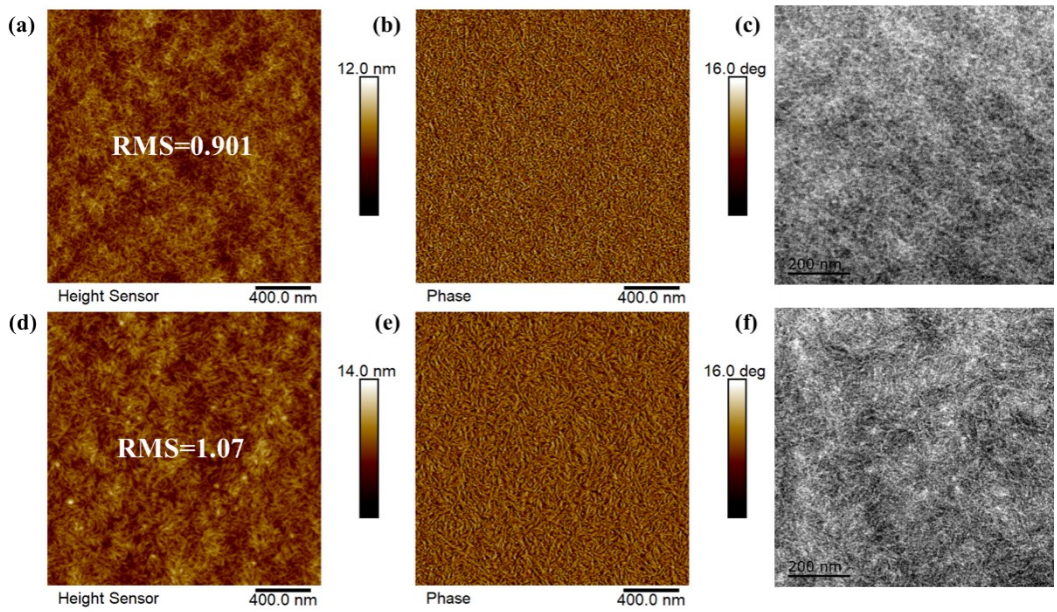

Fig. S4. Atomic force microscopy (AFM) height (right) and phase (middle) images, (a)(b)J71:IT-4Cl, (d)(e)J71:IT-2Cl; TEM images of (c)J71:IT-4Cl, (f) J71:IT-2Cl.

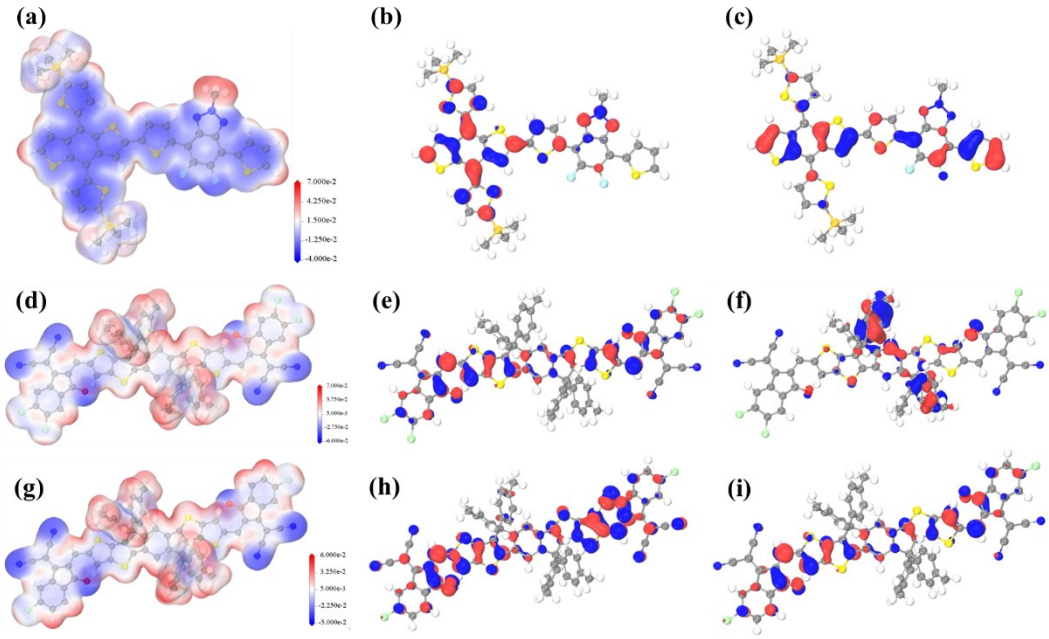

Fig. S5. Electrostatic Potential Surfaces of (a) J71, (d) IT-4Cl and (g) J71:IT-2Cl, molecular orbital electron densities HOMO and LUMO of (b)(c) J71, (e)(f) IT-4Cl and (h)(i) J71:IT-2Cl.

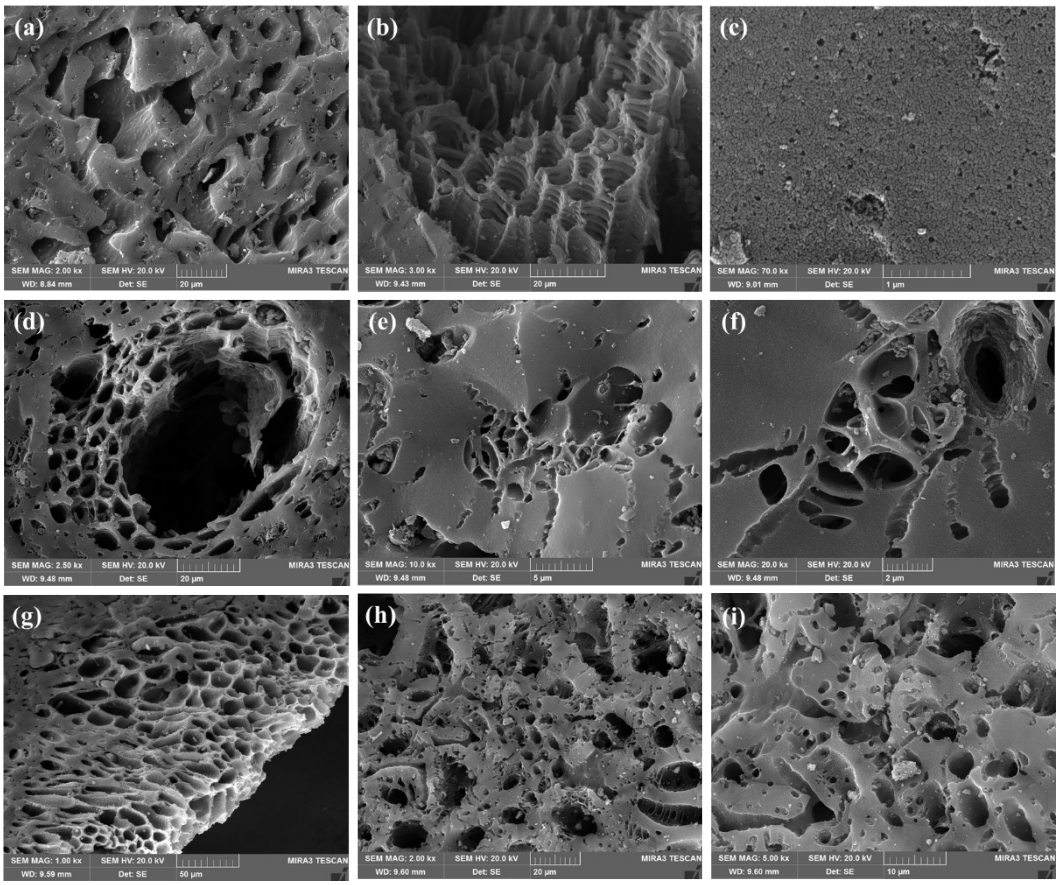

Fig. S6. SEM image of (a-c) CSC, (d-f) (J71:IT-4Cl)@CSC and (g-i) (J71:IT-2Cl)@CSC.

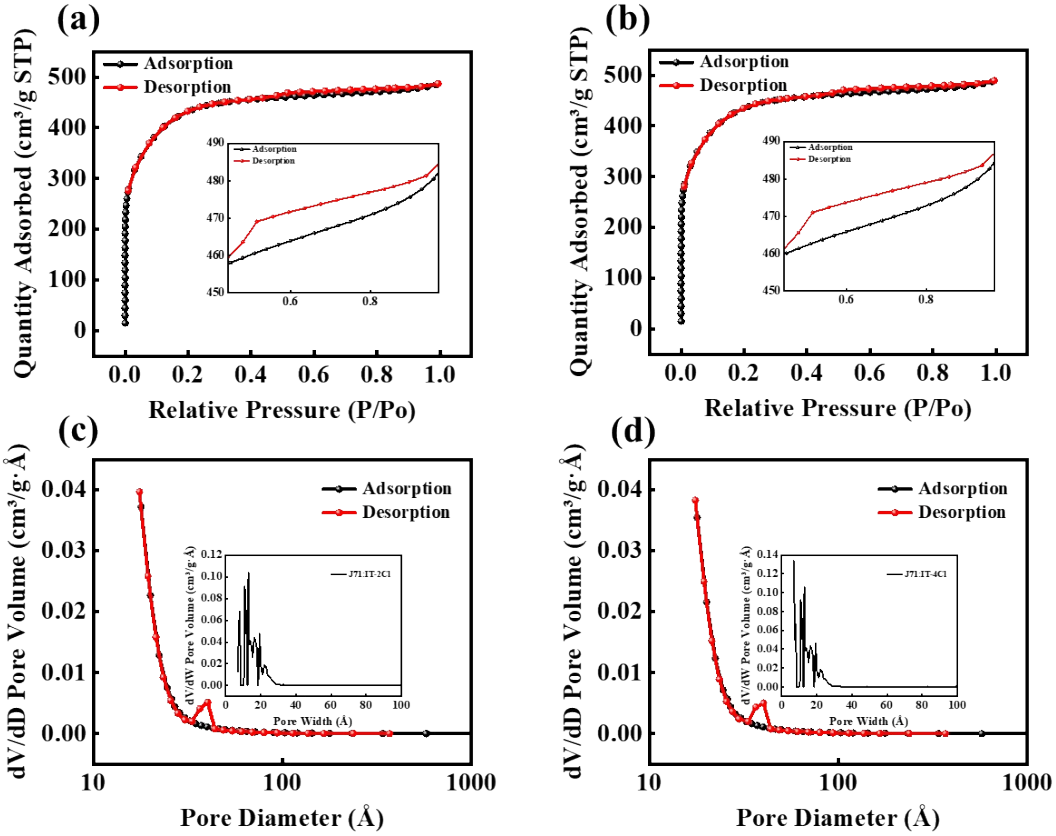

Fig. S7. N_2 adsorption-desorption isotherms of (a) (J71:IT-2Cl)@CSC and (b) (J71:IT-4Cl)@CSC; The pore size distribution curves of (c) (J71:IT-2Cl)@CSC and (d) (J71:IT-4Cl)@CSC.

Table. 1. N_2 adsorption-desorption properties of catalysts

	CSC	CSC@J71:IT-4Cl	CSC@J71:IT-2Cl
BET Surface Area	1,651.7533 m^2/g	1,241.8892 m^2/g	1,220.4820 m^2/g
Langmuir Surface Area	2,250.8275 m^2/g	2,084.9217 m^2/g	2,069.7172 m^2/g
Total Pore Volume	0.8157 cm^3/g	0.756949 cm^3/g	0.753021 cm^3/g
Micropore Volume	0.3468 cm^3/g	0.351325 cm^3/g	0.332876 cm^3/g
Average Pore Diameter	19.7534Å	24.381 Å	24.679 Å

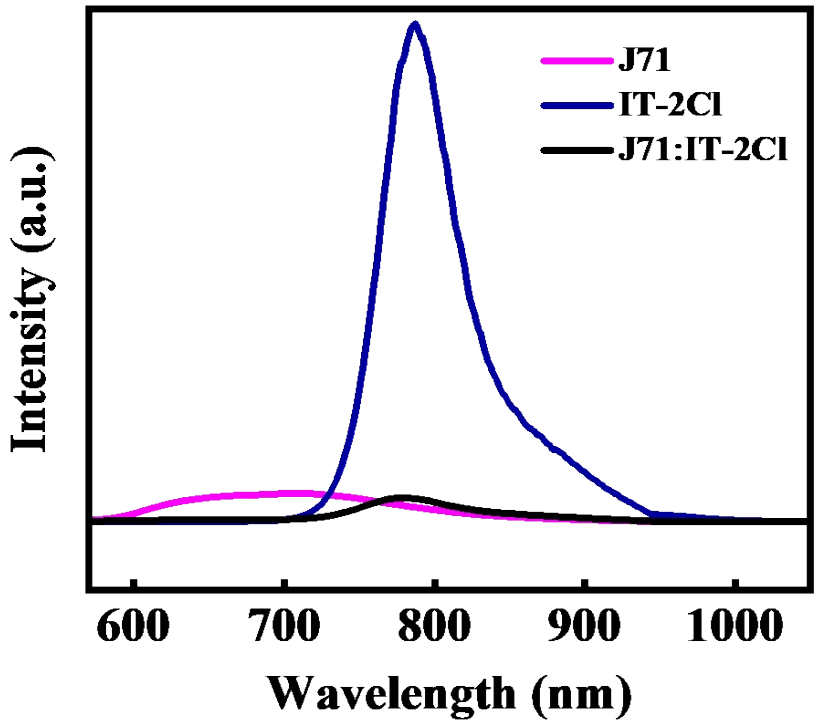

Fig. S8. PL spectra of J71, IT-2Cl and J71:IT-2Cl.

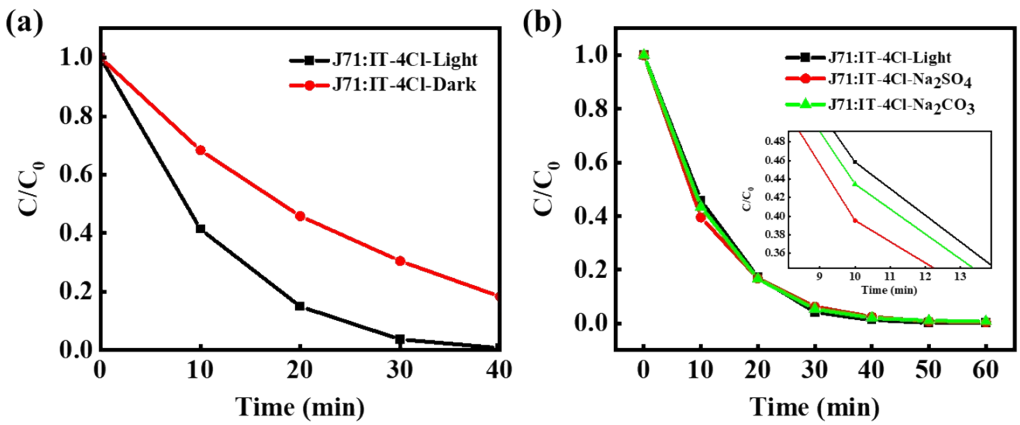

Fig. S9. (a) Photocatalytic degradation curves of SMX in the dark; (b) Effect of SO_4^{2-} and CO_3^{2-} on photocatalytic degradation of SMX (Reaction conditions: (J71:IT-4Cl)@CSC dosage = 100 mg, SMX = 20 mg·L^{-1}, pH = 7).

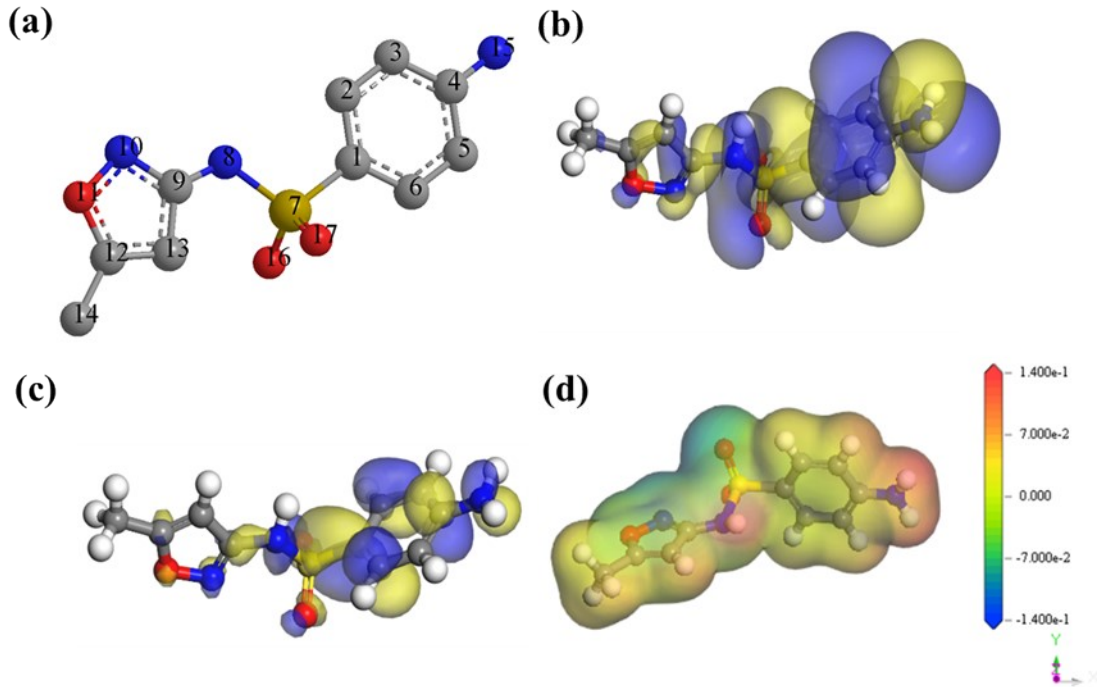

Fig. S10. (a) Structure and atomic numbering of SMX; molecular orbital electron densities (b) HOMO and (c) LUMO; (d) electrostatic potential distribution of SMX molecule.

Table. 2. Fukui function indices for SMX

No.	Atom	f^-	f^+	f^0
1	C	0.067	0.026	0.026
2	C	0.037	0.071	0.071
3	C	0.093	0.045	0.045
4	C	0.025	0.077	0.077
5	C	0.087	0.036	0.036
6	C	0.036	0.098	0.098
7	S	0.031	0.074	0.074
8	N	0.006	0.011	0.011
9	C	0.006	0.021	0.021
10	N	0.01	0.028	0.028
11	O	0.006	0.016	0.016
12	C	0.004	0.018	0.018
13	C	0.007	0.016	0.016
14	C	0.001	0.001	0.001
15	N	0.195	0.067	0.067
16	O	0.037	0.054	0.054
17	O	0.037	0.049	0.049

Table. 3. High resolution accurate mass data for SMX and Ps in negative ionization mode

Abbreviation name of Ps	Pseudo-Molecular Ion Formula	Structure	*m/z* $[m-H]^+$	Δ(ppm)	Retention time(min)
P1	$C_{10}H_{12}N_3O_5S$	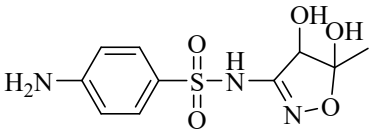	286.0492	0.0003	11.67
P2	$C_{10}H_{10}N_3O_4S$	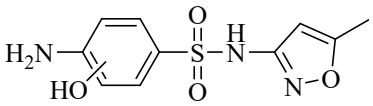	268.0386	0.0020	9.14
P4	$C_{10}H_8N_3O_4S$	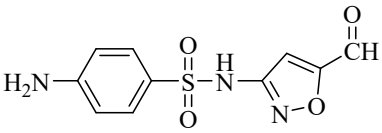	266.0230	0.0010	6.94
P5	$C_{10}H_8N_3O_5S$	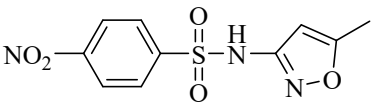	282.0179	0.0022	10.73
P6	$C_4H_5N_2O$	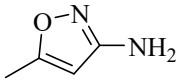	97.0396	-0.0002	9.79
P7	$C_6H_4NO_2S$	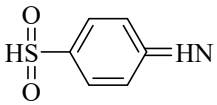	153.9957	-0.0021	9.40
P8	$C_8H_6N_3OS$	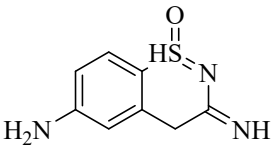	192.0226	-0.0017	13.92
P9	$C_8H_7N_3$	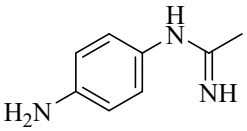	145.0634	0.00130	17.16
P10	$C_4H_5N_2O_4S$	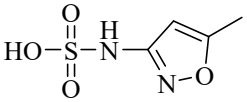	176.9964	-0.0036	14.28
P12	$C_7H_4N_3O_4S$	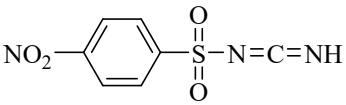	225.9917	0.0016	17.06
P13	C_6H_4NO	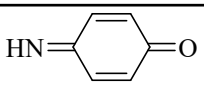	106.0287	-0.0074	1.12
P14	C_6H_4N	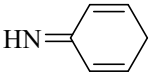	90.0338	-0.0006	15.87

Table. 4. High resolution accurate mass data for SMX and Ps in positive ionization mode

Abbreviation name of Ps	Pseudo-Molecular Ion Formula	Structure	*m/z* $[m-H]^+$	Δ(ppm)	Retention time(min)
P3	$C_{10}H_{11}N_2O_4S$	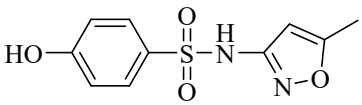	255.0434	-0.0017	5.72
P5	$C_{10}H_{10}N_3O_5S$	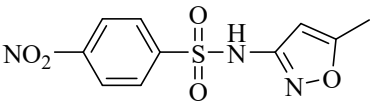	284.0335	0.0019	16.02
P6	$C_4H_7N_2O$	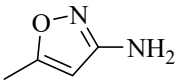	99.0552	0.0002	16.33
P7	$C_6H_6NO_2S$	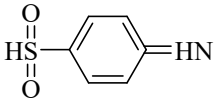	156.0113	-0.0370	0.22
P11	$C_6H_6NO_5S$	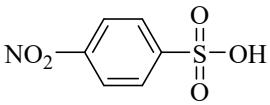	203.9961	-0.0245	0.19
P12	$C_7H_6N_3O_4S$	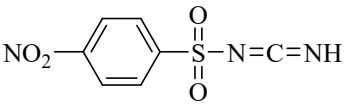	228.0073	0.0019	0.42

Table. 5. Predicted acute and chronic toxicity of SMX and its intermediates assessed via ECOSAR program

	Acure Toxicity			Chronic Toxicity		
	Fish	Daphnid	Green Algae	Fish	Daphnid	Green Algae
SMX	267	6.43	21.8	5	0.068	11.1
P1	4590	21.3	98.6	181	0.19	107
P2	8.75	0.927	1.56	0.09	0.188	0.275
P3	3.29	0.578	0.702	0.041	0.111	0.134
P4	282	330	145	146	2.25	37.9
P5	140	152	72.8	50	1.2	21.4
P6	270	3.63	13.8	6.59	0.036	9.16
P7	2.03E+8	6.08E+7	3.25E+6	9.34E+6	1.01E+6	2.06E+5
P8	961	9.09	36.8	27.5	0.087	28.7
P9	1890	10.1	45.5	70.2	0.091	46.2
P10	5.63E+5	1.39E+4	3.9E+4	2.92E+4	503	1.83E+4
P11	1.69E+6	7.06E+5	1.46E+5	1.15E+5	2.91E+4	1.93E+4
P12	22.7	20.2	3.39	0.381	4.13	2.79
P13	2.3E+3	2.62E+3	1.09E+3	1.43E+3	277	169
P14	72.5	41.3	31.1	7.11	4.05	8.18

Acute Toxicity

- **Not harmful**
- **Harmful**
- **Toxic**
- **Very toxic**

Chronic Toxicity

- **Not harmful**
- **Harmful**
- **Toxic**
- **Very toxic**

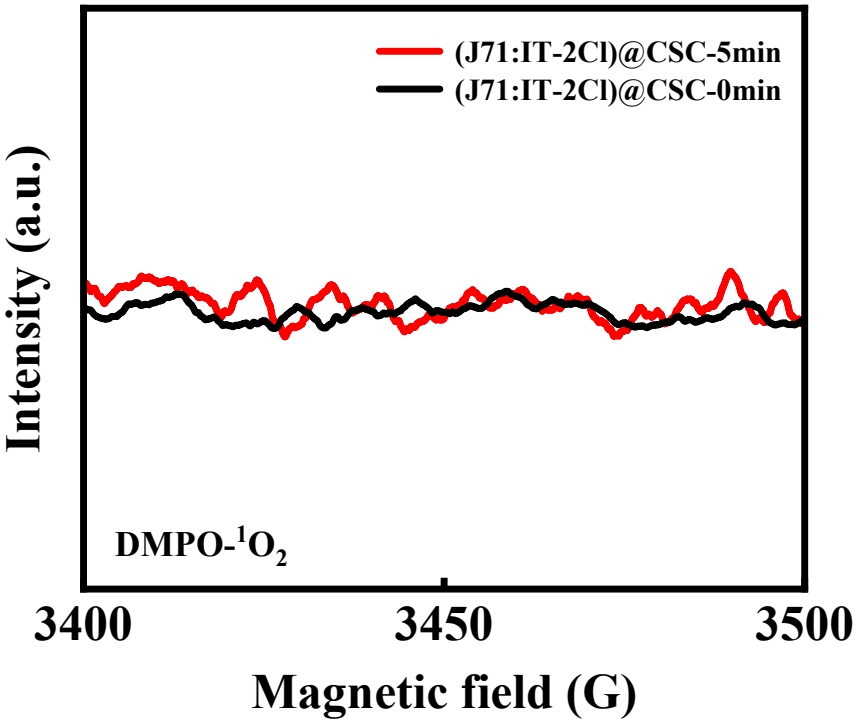

Fig. S11. ESR trapping spectra of $^1O_2$.

Table. 6. SXM removal by different photocatalysts

Catalyst	SMX (mg L^{-1})	Removal efficiency (%)	Reaction time (min)	References
(J71:IT-4Cl)@CSC	20	> 99	60	This work
ZnO@g-C_3N_4	30	> 99	90	2
WO_3	50	99	180	3
AgBr-$BaMoO_4$	10	64	75	4
N-SrTiO/NHVO	40	90	120	5
CaCuTiO	20	99	90	6
Fe_2O_3/Co_3O_4@NF	80	100	150	7
3D-10 %-WO_3-UiO-66@rGO	20	90.39	60	8
CAU-17-st-8h	15	75.1	300	9
HBBT	5	82.3	30	10
FeCoNiCuZn	5	97	90	11
SAAg/CN/Vis-PI		100	25	12
Fc@rGO-ZnO	20	>90	180	13

References

1. Zhang, H.; Yao, H.; Hou, J.; Zhu, J.; Zhang, J.; Li, W.; Yu, R.; Gao, B.; Zhang, S.; Hou, J., Over 14% Efficiency in Organic Solar Cells Enabled by Chlorinated Nonfullerene Small-Molecule Acceptors. *Advanced Materials* **2018,** *30* (28), 1800613.
2. Mirzaei, A.; Yerushalmi, L.; Chen, Z.; Haghighat, F., Photocatalytic degradation of sulfamethoxazole by hierarchical magnetic ZnO@g-C3N4: RSM optimization, kinetic study, reaction pathway and toxicity evaluation. *Journal of Hazardous Materials* **2018,** *359*, 516-526.
3. Beheshti, F.; M. A. Tehrani, R.; Khadir, A., Sulfamethoxazole removal by photocatalytic degradation utilizing TiO2 and WO3 nanoparticles as catalysts: analysis of various operational parameters. *International Journal of Environmental Science and Technology* **2019,** *16* (12), 7987-7996.
4. Ray, S. K.; Dhakal, D.; Lee, S. W., Insight into sulfamethoxazole degradation, mechanism, and pathways by AgBr-BaMoO4 composite photocatalyst. *Journal of Photochemistry and Photobiology A: Chemistry* **2018,** *364*, 686-695.
5. Zhang, Y.; Li, Y.; Yuan, Y., Enhanced sulfamethoxazole photodegradation by N-SrTiO3/NH4V4O10 S-scheme photocatalyst: DFT calculation and photocatalytic mechanism insight. *Journal of Colloid and Interface Science* **2023,** *645*, 860-869.
6. Lien, E.; Sahu, R. S.; Chen, W.-L.; Shih, Y.-h., Effective photocatalytic degradation of sulfamethoxazole using tunable CaCu3Ti4O7 perovskite. *Chemosphere* **2022,** *294*, 133744.
7. Qiu, J.; Yue, C.; Zheng, W.; Liu, F.; Zhu, J., Enhanced photocatalytic degradation of sulfamethoxazole by stable hierarchical Fe2O3/Co3O4 heterojunction on nickel foam. *Chinese Chemical Letters* **2021,** *32* (11), 3431-3434.
8. Huong, V. T.; Duc, B. V.; An, N. T.; Anh, T. T. P.; Aminabhavi, T. M.; Vasseghian, Y.; Joo, S.-W., 3D-Printed WO3-UiO-66@reduced graphene oxide nanocomposites for photocatalytic degradation of sulfamethoxazole. *Chemical Engineering Journal* **2024,** *483*, 149277.
9. Pham, H. A. L.; Nguyen, V. H.; Lee, T.; Nguyen, V. C.; Nguyen, T. D., Construction of BiOCl/bismuth-based halide perovskite heterojunctions derived from the metal-organic framework CAU-17 for effective photocatalytic degradation. *Chemosphere* **2024,** *357*, 142114.
10. Liu, G.; Fei, H.; Feng, Z.; Shao, Q.; Zhao, T.; Guo, W.; Li, F., Tri-phase interface to enhance the performance of piezoelectric photocatalysis and recyclability of hydrophobic BiOI/BaTiO3 heterojunction. *Journal of Cleaner Production* **2024,** *440*, 140886.
11. Das, S.; Kumar, S.; Sarkar, S.; Pradhan, D.; Tiwary, C. S.; Chowdhury, S., High entropy spinel oxide nanoparticles for visible light-assisted photocatalytic degradation of binary mixture of antibiotic pollutants in different water matrixes. *Journal of Materials Chemistry A* **2024,** *12* (27), 16815-16830.
12. Dou, L.; Huang, W.; Huang, Y.; Liu, C.; Li, N.; Li, J.; Lai, B., Single-atom Ag porous tubular carbon nitride photocatalyst with N-vacancies as efficient visible-light periodate activator: Performance and mechanism. *Chemical Engineering Journal* **2024**, 158796.
13. Roy, N.; Kannabiran, K.; Mukherjee, A., Integrated adsorption and photocatalytic degradation based removal of ciprofloxacin and sulfamethoxazole antibiotics using Fc@rGO-ZnO nanocomposite in aqueous systems. *Chemosphere* **2023,** *333*, 138912.